

Rare B-Meson Decays at the Crossroads *

Ahmed Ali*

Deutsches Elektronen-Synchritron DESY

D-22607 Hamburg, Germany

**E-mail: ahmed.ali@desy.de*

Experimental era of rare B -decays started with the measurement of $B \rightarrow K^* \gamma$ by CLEO in 1993, followed two years later by the measurement of the inclusive decay $B \rightarrow X_s \gamma$, which serves as the standard candle in this field. The frontier has moved in the meanwhile to the experiments at the LHC, in particular, LHCb, with the decay $B^0 \rightarrow \mu^+ \mu^-$ at about 1 part in 10^{10} being the smallest branching fraction measured so far. Experimental precision achieved in this area has put the standard model to unprecedented stringent tests and more are in the offing in the near future. I review some key measurements in radiative, semileptonic and leptonic rare B -decays, contrast them with their estimates in the SM, and focus on several mismatches reported recently. They are too numerous to be ignored, yet, standing alone, none of them is significant enough to warrant the breakdown of the SM. Rare B -decays find themselves at the crossroads, possibly pointing to new horizons, but quite likely requiring an improved theoretical description in the context of the SM. An independent precision experiment such as Belle II may help greatly in clearing some of the current experimental issues.

Keywords: Standard Model, Flavour Physics, Rare B Decays, LHC, Anomalies.

1. Introduction

The interest in studying rare B decays is immense. This is due to the circumstance that these decays, such as $b \rightarrow (s, d) \gamma$, $b \rightarrow (s, d) \ell^+ \ell^-$, are flavour-changing-neutral-current (FCNC) processes, involving the quantum number transitions $|\Delta B| = 1, |\Delta Q| = 0$. In the SM¹, they are not allowed at the tree level, but are induced by loops and are governed by the GIM (Glashow-Iliopoulos-Maiani) mechanism², which imparts them sensitivity to higher masses, (m_t, m_W) . As a consequence, they determine the CKM³ (Cabibbo-Kobayashi-Maskawa) matrix elements. Of these, the elements in the third row, V_{td} , V_{ts} and V_{tb} are of particular interest. While $|V_{tb}|$ has been measured in the production and decays of the top quarks in hadronic collisions⁴, the first two are currently not yet directly accessible. In the SM, these CKM matrix elements have been indirectly determined from the $B^0 - \bar{B}^0$ and $B_s^0 - \bar{B}_s^0$ mixings. Rare B -decays provide independent measurements of the same quantities.

In theories involving physics beyond the SM (BSM), such as the 2-Higgs doublet models or supersymmetry, transitions involving the FCNC processes are sensitive to

*To be published in the Proceedings of the Conference on New Physics at the Large Hadron Collider, Nanyang Technological University, Singapore. 29 February - 4 March, 2016.

the masses and couplings of the new particles. Precise experiments and theory are needed to establish or definitively rule out the BSM effects. Powerful calculation techniques, such as the heavy quark effective theory (HQET)⁵ and the soft collinear effective theory (SCET)^{6–8} have been developed to incorporate power $1/m_c$ and $1/m_b$ corrections to the perturbative QCD estimates. More importantly, they enable a better theoretical description by separating the various scales involved in B decays and in establishing factorisation of the decay matrix elements. In exclusive decays, one also needs the decay form factors and a lot of theoretical progress has been made using the lattice QCD⁹ and QCD sum rule techniques^{10–13}, often complementing each other, as they work best in the opposite q^2 -ranges. It is this continued progress in QCD calculational framework, which has taken us to the level of sophistication required to match the experimental advances.

In this paper, I review what, in my view, are some of the key measurements in the radiative, semileptonic and leptonic rare B -decays and confront them with the SM-based calculations, carried out with the theoretical tools just mentioned. However, this is not a comprehensive review of this subject, but the hope is that the choice of topics reflects both the goals achieved in explaining some landmark measurements and focus on open issues. In section 2, I review the inclusive and some exclusive radiate rare B -decays. There are no burning issues in this area - at least not yet. In section 3, the corresponding inclusive and exclusive semileptonic decays are taken up. Again, there are no open issues in the inclusive semileptonic decays, but experimental precision is limited currently, which is bound to improve significantly at Belle II. There are, however, a lot of open issues in the exclusive semileptonic decays, in particular in R_K , the ratio of the decay widths for $B \rightarrow K\mu^+\mu^-$ and $B \rightarrow Ke^+e^-$, hinting at the possible breakdown of lepton universality, the linchpin of the SM, reviving the interest in low-mass leptoquarks. One should also mention here similar issues in tree-level semileptonic decays, such as $R_D^{\tau/\ell}$ and $R_{D^*}^{\tau/\ell}$, the ratios involving the decays $B \rightarrow D^{(*)}\tau\nu_\tau$ and $B \rightarrow D^{(*)}\ell\nu_\ell$ ($\ell = e, \mu$). There are also other dissenting areas, which go by the name of P_5' -anomaly, which is a certain coefficient in the angular description of the decay $B \rightarrow K^*\mu^+\mu^-$, which presumably need a better theoretical (read QCD) description than is available at present. They are discussed in section 3. In section 4, we discuss the CKM-suppressed $b \rightarrow d\ell^+\ell^-$ decays, which is a new experimental frontier initiated by the LHCb measurements of the branching fraction and the dimuon invariant mass distribution in the decay $B^\pm \rightarrow \pi^\pm\mu^+\mu^-$. Finally, the rarest B - and B_s -decays measured so far, $B \rightarrow \mu^+\mu^-$ and $B_s \rightarrow \mu^+\mu^-$, are taken up in section 5. Current measurements also show some (mild) deviations in their branching ratios versus the SM. A representative global fit of the data on the semileptonic and leptonic rare B -decays in terms of the Wilson coefficients from possible new physics is shown in section 6. Some concluding remarks are made in section 7.

2. Rare Radiative B -decays in the SM and Experiments

In 1993, the CLEO collaboration at the Cornell e^+e^- collider measured the decay $B \rightarrow K^*\gamma$ ¹⁴, initiating the field of rare B -decays, followed two years later by the measurement of the inclusive decay $B \rightarrow X_s\gamma$ ¹⁵. The branching ratio ($B \rightarrow K^*\gamma$) = $(4.5 \pm 1.5 \pm 0.9) \times 10^{-5}$ was in agreement with the SM estimates, but theoretical uncertainty was large. Measuring the Inclusive process $B \rightarrow X_s\gamma$ was challenging, but as the photon energy spectrum in this process was already calculated in 1990 by Christoph Greub and me¹⁶, this came in handy for the CLEO measurements¹⁷ shown in Fig. 1 (left frame) and compared with the theoretical prediction¹⁶. Since then, a lot of experimental and theoretical effort has gone in the precise measurements and in performing higher order perturbative and non-perturbative calculations. As a consequence, $B \rightarrow X_s\gamma$ has now become the standard candle of FCNC processes, with the measured branching ratio and the precise higher order SM-based calculation providing valuable constraints on the parameters of BSM physics. The impact of the B -factories on this measurement can be judged by the scale in Fig. 1 (right frame), which is due to the Belle collaboration¹⁸.

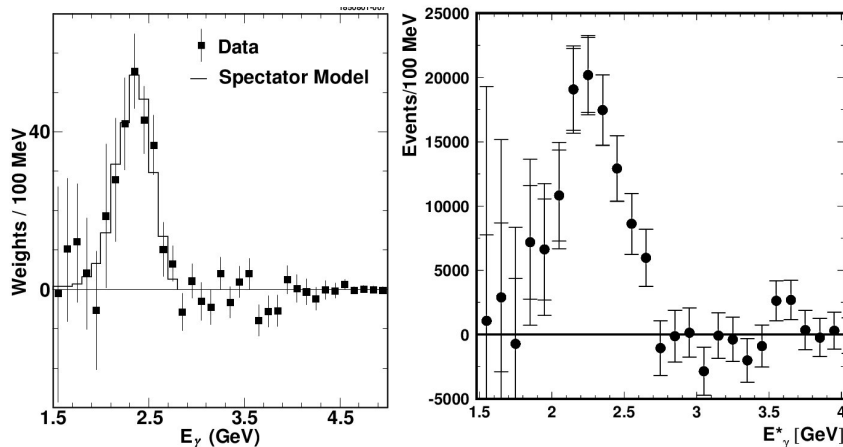


Fig. 1. Photon energy spectrum in the inclusive decay $B \rightarrow X_s\gamma$ measured by CLEO (left frame)¹⁷ and Belle (right frame)¹⁸.

The next frontier of rare B -decays involves the so-called electroweak penguins, which govern the decays of the inclusive processes $B \rightarrow (X_s, X_d)\ell^+\ell^-$ and the exclusive decays such as $B \rightarrow (K, K^*, \pi)\ell^+\ell^-$. These processes have rather small branching ratios and hence they were first measured at the B -factories. Inclusive decays remain their domain, but experiments at the LHC, in particular, LHCb, are now at the forefront of exclusive semileptonic decays. Apart from these, also the leptonic B -decays $B_s \rightarrow \mu^+\mu^-$ and $B_d \rightarrow \mu^+\mu^-$ have been measured at the LHC.

I will review some of the key measurements and the theory relevant for their

interpretation. This description is anything but comprehensive, for which I refer to some recent excellent references^{19–22} and resources, such as HFAG²³ and FLAG⁹.

2.1. Inclusive decays $B \rightarrow X_s \gamma$ at NNLO in the SM

The leading order diagrams for the decay $b \rightarrow s \gamma$ are shown in Fig. 2, including also the tree diagram for $b \rightarrow u \bar{u} s \gamma$, which yields a soft photon. The first two diagrams are anyway suppressed due to the CKM matrix elements, as indicated. The charm- and top- quark contributions enter with opposite signs, and the relative contributions indicated are after including the leading order (in α_s) QCD effects. A typical diagram depicting perturbative QCD corrections due to the exchange of a gluon is also shown.

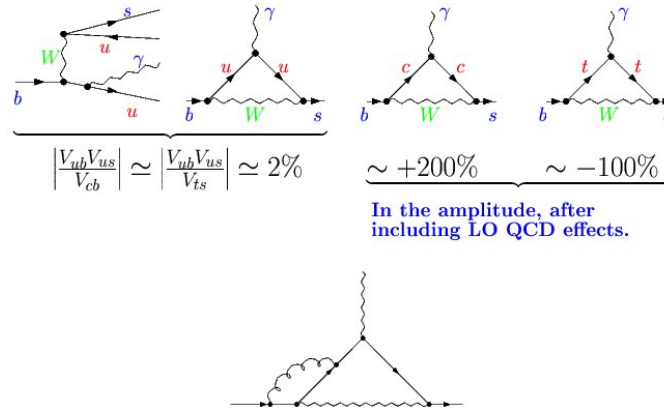


Fig. 2. Examples of the leading electroweak diagrams for $B \rightarrow X_s \gamma$ from the up, charm, and top quarks. A diagram involving a gluon exchange is shown in the lower figure.

The QCD logarithms $\alpha_s \ln M_W^2/m_b^2$ enhance the branching ratio $\mathcal{B}(B \rightarrow X_s \gamma)$ by more than a factor 2, and hence such logs have to be resummed. This is done using an effective field theory approach, obtained by integrating out the top quark and the W^\pm bosons. Keeping terms up to dimension-6, the effective Lagrangian for $B \rightarrow X_s \gamma$ and $B \rightarrow X_s \ell^+ \ell^-$ reads as follows:

$$\mathcal{L} = \mathcal{L}_{QCD \times QED}(q, l) + \frac{4G_F}{\sqrt{2}} V_{ts}^* V_{tb} \sum_{i=1}^{10} C_i(\mu) O_i$$

($q = u, d, s, c, b$, $l = e, \mu, \tau$)

$$O_i = \begin{cases} (\bar{s}\Gamma_i c)(\bar{c}\Gamma'_i b), & i = 1, (2), & C_i(m_b) \sim -0.26 \quad (1.02) \\ (\bar{s}\Gamma_i b)\Sigma_q(\bar{q}\Gamma'_i q), & i = 3, 4, 5, 6, & |C_i(m_b)| < 0.08 \\ \frac{em_b}{16\pi^2}\bar{s}_L\sigma^{\mu\nu}b_R F_{\mu\nu}, & i = 7, & C_7(m_b) \sim -0.3 \\ \frac{gm_b}{16\pi^2}\bar{s}_L\sigma^{\mu\nu}T^a b_R G_{\mu\nu}^a, & i = 8, & C_8(m_b) \sim -0.16 \\ \frac{e^2}{16\pi^2}(\bar{s}_L\gamma_\mu b_L)(\bar{l}\gamma^\mu(\gamma_5)l), & i = 9, (10) & C_i(m_b) \sim 4.27 \quad (-4.2) \end{cases}$$

Here, G_F is the Fermi coupling constant, V_{ij} are the CKM matrix elements, O_i are the four-Fermi and dipole operators, and $C_i(\mu)$ are the Wilson coefficients, evaluated at the scale μ , which is taken typically as $\mu = m_b$, and their values in the NNLO accuracy are given above for $\mu = 4.8$ GeV. Variations due to a different choice of μ and uncertainties from the upper scale-setting $m_t/2 \leq \mu_0 \leq 2m_t$ can be seen elsewhere¹⁹.

There are three essential steps of the calculation:

- **Matching:** Evaluating $C_i(\mu_0)$ at $\mu_0 \sim M_W$ by requiring the equality of the SM and the effective theory Green functions.
- **Mixing:** Deriving the effective theory renormalisation group equation (RGE) and evolving $C_i(\mu)$ from μ_0 to $\mu_b \sim m_b$.
- **Matrix elements:** Evaluating the on-shell amplitudes at $\mu_b \sim m_b$.

All three steps have been improved in perturbation theory and now include the next-to-next-to-leading order effects (NNLO), i.e., contributions up to $O(\alpha_s^2(m_b))$. A monumental theoretical effort stretched well over a decade with the participation of a large number of theorists underlies the current theoretical precision of the branching ratio. The result is usually quoted for a threshold photon energy to avoid experimental background from other Bremsstrahlung processes. For the decay with $E_\gamma > 1.6$ GeV in the rest frame of the B meson, the result at NNLO accuracy is^{24,25}

$$\mathcal{B}(B \rightarrow X_s \gamma) = (3.36 \pm 0.23) \times 10^{-4}, \quad (1)$$

where the dominant SM uncertainty is non-perturbative²⁶. This is to be compared with the current experimental average of the same²³

$$\mathcal{B}(B \rightarrow X_s \gamma) = (3.43 \pm 0.21 \pm 0.07) \times 10^{-4}, \quad (2)$$

where the first error is statistical and the second systematic, yielding a ratio 1.02 ± 0.08 , providing a test of the SM to an accuracy better than 10%.

The CKM-suppressed decay $B \rightarrow X_d \gamma$ has also been calculated in the NNLO precision. The result for $E_\gamma > 1.6$ GeV is²⁴

$$\mathcal{B}(B \rightarrow X_d \gamma) = (1.73^{+0.12}_{-0.22}) \times 10^{-5}. \quad (3)$$

This will be measured precisely at Belle II. The constraints on the CP asymmetry are not very restrictive, but the current measurements are in agreement with the SM expectation. For further details, see HFAG²³.

2.2. Bounds on the charged Higgs mass from $\mathcal{B}(B \rightarrow X_s \gamma)$

As the agreement between the SM and data is excellent, the decay rate for $B \rightarrow X_s \gamma$ provides constraints on the parameters of the BSM theories, such as supersymmetry and the 2 Higgs-doublet models (2HDM). In calculating the BSM effects, depending on the model, the SM operator basis may have to be enlarged, but in many cases one anticipates additive contributions to the Wilson coefficients in the SM basis. In the context of $B \rightarrow X_s \gamma$, it is customary to encode the BSM effects in the Wilson coefficients of the dipole operators $C_7(\mu)$ and $C_8(\mu)$, and the constraints from the branching ratio on the additive coefficients ΔC_7 and ΔC_8 then takes the numerical form²⁴

$$\mathcal{B}(B \rightarrow X_s \gamma) \times 10^4 = (3.36 \pm 0.23) - 8.22\Delta C_7 - 1.99\Delta C_8. \quad (4)$$

To sample the kind of constraints that can be derived on the parameters of the BSM models, the 2HDM is a good case, as the branching ratio for the decay $B \rightarrow X_s \gamma$ in this model has been derived to the same theoretical accuracy²⁸. The Lagrangian for the 2HDM is

$$\mathcal{L}_{H^\pm} = (2\sqrt{2}G_F)^{1/2} \sum_{i,j=1}^3 \bar{u}_i (A_u m_{u_i} V_{ij} P_L - A_d m_{d_j} V_{ij} P_R) d_j H^\pm + h.c., \quad (5)$$

where V_{ij} are the CKM matrix elements and $P_{L/R} = (1 \mp \gamma_5)/2$. The 2HDM contributions to the Wilson coefficients are proportional to $A_i A_j^*$, representing the contributions from the up-type A_u and down-type A_d quarks. They are defined in terms of the ratio of the vacuum expectation values, called $\tan \beta$, and are model dependent.

- 2HDM of type-I: $A_u = A_d = \frac{1}{\tan \beta}$,
- 2HDM of type-II: $A_u = -1/A_d = \frac{1}{\tan \beta}$.

Examples of Feynman diagrams contributing to $B \rightarrow X_s \gamma$ in the 2HDM are shown in Fig. 3. Apart from $\tan \beta$, the other parameter of the 2HDM is the mass of the charged Higgs M_H^\pm . As $\mathcal{B}(B \rightarrow X_s \gamma)$ becomes insensitive to $\tan \beta$ for larger values, $\tan \beta > 2$, the 2HDM contribution depends essentially on M_H^\pm . The current measurements and the SM estimates then provide constraints on M_H^\pm , as shown in Fig. 4, ^a updated using^{24,28}, yielding²⁴ $M_H^\pm > 480$ GeV (90% C.L.) and $M_H^\pm > 358$ GeV (99% C.L.). These constraints are competitive to the direct searches of the H^\pm at the LHC.

^aI thank Matthias Steinhauser for providing this figure.

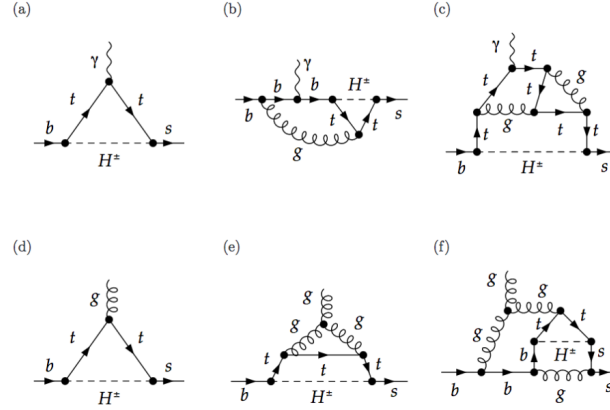


Fig. 3. Sample Feynman diagrams that matter for $B \rightarrow X_s \gamma$ in the 2HDM²⁸. H^\pm denotes a charged Higgs.

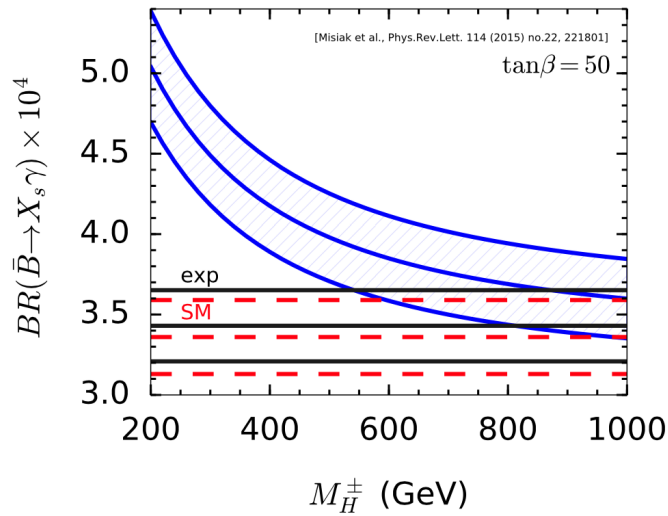


Fig. 4. Constraints on the charged Higgs mass m_H^\pm from $\mathcal{B}(B \rightarrow X_s \gamma)$ in the 2HDM^{24,28}. Measured branching ratio (exp) and the SM estimates are also shown. The curves demarcate the central values and $\pm 1\sigma$ errors.

2.3. Exclusive radiative rare B decays

Exclusive radiative decays, such as $B \rightarrow V \gamma$ ($V = K^*, \rho, \omega$) and $B_s \rightarrow \phi \gamma$, have been well-measured at the B factories. In addition, they offer the possibility of measuring CP- and isospin asymmetries, a topic I will not discuss here. Theoretically, exclusive decays are more challenging, as they require the knowledge of the form factors at $q^2 = 0$, which can not be calculated directly using Lattice QCD. However,

light-cone QCD sum rules^{12,13} also do a good job for calculating heavy \rightarrow light form factors at low- q^2 . In addition, the matrix elements require gluonic exchanges between the spectator quark and the active quarks (spectator-scattering), introducing intermediate scales in the decay rates. Also long-distance effects generated by the four-quark operators with charm quarks are present and are calculable in limited regions²⁹. Thus, exclusive decays are theoretically not as precise as the inclusive decay $B \rightarrow X_s \gamma$. However, techniques embedded in HQET and SCET have led to the factorisation of the decay matrix elements into perturbatively calculable (hard) and non-perturbative (soft) parts, akin to the deep inelastic scattering processes. These factorisation-based approaches are the main work-horse in this field. Renormalisation group (RG) methods then allow to sum up large logarithms, and this program has been carried out to a high accuracy.

A detailed discussion of the various techniques requires a thorough review, which can't be carried out here. I will confine myself by pointing to some key references, beginning from the QCD factorisation approach, pioneered by Beneke, Buchalla, Neubert and Sachrajda³⁰, which has been applied to the radiative decays $B \rightarrow (K^*, \rho, \omega) \gamma$ ³¹⁻³⁴. Another theoretical framework, called pQCD^{35,36}, has also been put to use in these decays^{37,38}. The SCET-based methods have also been harnessed^{39,40}. The advantage of SCET is that it allows for an unambiguous separation of the scales, and an operator definition of each object in the factorisation formula can be given. Following the QCD factorisation approach, a factorisation formula for the $B \rightarrow V \gamma$ matrix element can be written in SCET as well

$$\langle V \gamma | Q_i | B \rangle = \Delta_i C^A \xi_{V_\perp} + \frac{\sqrt{m_B} F f_{V_\perp}}{4} \int dw du \phi_+^B(w) \phi_\perp^V(u) t_i^{II}, \quad (6)$$

where F and f_{V_\perp} are meson decay constants; $\phi_+^B(w)$ and $\phi_\perp^V(u)$ are the light-cone distribution amplitudes for the B - and V -meson, respectively. The SCET form factor ξ_{V_\perp} is related to the QCD form factor through perturbative and power corrections, and the perturbative hard QCD kernels are the coefficients $\Delta_i C^A$ and t_i^{II} . They are known to complete NLO accuracy in RG-improved perturbation theory⁴⁰.

The factorisation formula (6) has been calculated to NNLO accuracy in SCET⁴¹ (except for the NNLO corrections from the spectator scattering). As far as the decays $B \rightarrow K^* \gamma$ and $B_s \rightarrow \phi \gamma$ are concerned, the partial NNLO theory is still the state-of-the-art. Their branching ratios as well as the ratio of the decay rates $\mathcal{B}(B_s \rightarrow \phi \gamma) / \mathcal{B}(B \rightarrow K^* \gamma)$ are given in Table 1, together with the current experimental averages²³. The corresponding calculations for the CKM-suppressed decays $B \rightarrow (\rho, \omega) \gamma$ are not yet available to the desired theoretical accuracy, due to the annihilation contributions, for which, to the best of my knowledge, no factorisation theorem of the kind discussed above has been proven. The results from a QCD-Factorisation based approach³² for $B \rightarrow \rho \gamma$ are also given in Table 1 and compared with the data. The exclusive decay rates shown are in agreement with the experimental measurements, though theoretical precision is not better than 20%. Obviously, there is need for a better theoretical description, more so as Belle II will

measure the radiative decays with greatly improved precision. I will skip a discussion of the isospin and CP asymmetries in these decays, as the current experimental bounds²³ are not yet probing the SM in these observables.

Table 1. Measurements [HFAG 2014]²³ and SM-based estimates of $\mathcal{B}(B \rightarrow (K^*, \rho)\gamma)$ and $\mathcal{B}(B_s \rightarrow \phi\gamma)$ in units of 10^{-5} , and the ratio $\mathcal{B}(B_s \rightarrow \phi\gamma)/\mathcal{B}(B^0 \rightarrow K^{*0}\gamma)$.

Decay Mode	Expt. (HFAG)	Theory (SM)
$B^0 \rightarrow K^{*0}\gamma$	4.33 ± 0.15	4.6 ± 1.4
$B^+ \rightarrow K^{*+}\gamma$	4.21 ± 0.18	4.3 ± 1.4
$B_s \rightarrow \phi\gamma$	3.59 ± 0.36	4.3 ± 1.4
$B_s \rightarrow \phi\gamma/B^0 \rightarrow K^{*0}\gamma$	0.81 ± 0.08	1.0 ± 0.2
$B^0 \rightarrow \rho^0\gamma$	$0.86^{+0.15}_{-0.14}$	0.65 ± 0.12
$B^+ \rightarrow \rho^+\gamma$	0.98 ± 0.25	1.37 ± 0.26

3. Semileptonic $b \rightarrow s$ decays $B \rightarrow (X_s, K, K^*)\ell^+\ell^-$

There are two $b \rightarrow s$ semileptonic operators in SM:

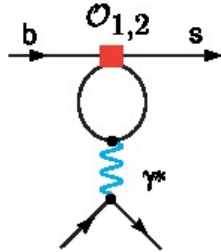
$$O_i = \frac{e^2}{16\pi^2} (\bar{s}_L \gamma_\mu b_L) (\bar{l} \gamma^\mu (\gamma_5) l), \quad i = 9, (10)$$

Their Wilson Coefficients have the following perturbative expansion:

$$C_9(\mu) = \frac{4\pi}{\alpha_s(\mu)} C_9^{(-1)}(\mu) + C_9^{(0)}(\mu) + \frac{\alpha_s(\mu)}{4\pi} C_9^{(1)}(\mu) + \dots$$

$$C_{10} = C_{10}^{(0)} + \frac{\alpha_s(M_W)}{4\pi} C_{10}^{(1)} + \dots$$

The term $C_9^{(-1)}(\mu)$ reproduces the electroweak logarithm that originates from the photonic penguins with charm quark loops, shown below⁴².



The first two terms in the perturbative expansion of $C_9(m_b)$ are

$$C_9^{(0)}(m_b) \simeq 2.2; \quad \frac{4\pi}{\alpha_s(m_b)} C_9^{(-1)}(m_b) = \frac{4}{9} \ln \frac{M_W^2}{m_b^2} + \mathcal{O}(\alpha_s) \simeq 2.$$

As they are very similar in magnitude, one needs to calculate the NNLO contribution to get reliable estimates of the decay rate. In addition, leading power corrections in $1/m_c$ and $1/m_b$ are required.

3.1. Inclusive semileptonic decays $B \rightarrow X_s \ell^+ \ell^-$

A lot of theoretical effort has gone into calculating the perturbative QCD NNLO, electromagnetic logarithms and power corrections^{42–46}. The B-factory experiments Babar and Belle have measured the dilepton invariant mass spectrum $d\mathcal{B}(B \rightarrow X_s \ell^+ \ell^-)/dq^2$ practically in the entire kinematic region and have also measured the so-called Forward-backward lepton asymmetry $A_{FB}(q^2)$ ⁴⁷. They are shown in Fig. 5, and compared with the SM-based theoretical calculations. Note that a cut of $q^2 > 0.2 \text{ GeV}^2$ on the dilepton invariant squared mass is used. As seen in these figures, two resonant regions near $q^2 = M_{J/\psi}^2$ and $q^2 = M_{J/\psi'}^2$ have to be excluded when comparing with the short-distance contribution. They make up what is called the long-distance contribution from the processes $B \rightarrow X_s + (J/\psi, J/\psi') \rightarrow X_s + \ell^+ \ell^-$, whose dynamics is determined by the hadronic matrix elements of the operators O_1 and O_2 . They have also been calculated via a dispersion relation⁴⁸ and data on the measured quantity $R_{\text{had}}(s) = \sigma(e^+e^- \rightarrow \text{hadrons})/\sigma(e^+e^- \rightarrow \mu^+\mu^-)$, and in some analyses are also included. As the (short-distance) contribution is expected to be a smooth function of q^2 , one uses the perturbative distributions in interpolating these regions as well. The experimental distributions are in agreement with the SM, including also the zero point of $A_{FB}(q^2)$, which is a sensitive function of the ratio of the two Wilson coefficients C_9 and C_{10} .

The branching ratio for the inclusive decay $B \rightarrow X_s \ell^+ \ell^-$ with a lower cut on the dilepton invariant mass $q^2 > 0.2 \text{ GeV}^2$ at NNLO accuracy is⁴⁴

$$\mathcal{B}(B \rightarrow X_s \ell^+ \ell^-) = (4.2 \pm 0.7) \times 10^{-6}, \quad (7)$$

to be compared with the current experimental average of the same²³

$$\mathcal{B}(B \rightarrow X_s \ell^+ \ell^-) = (3.66_{-0.77}^{+0.76}) \times 10^{-6}. \quad (8)$$

The two agree within theoretical and experimental errors. The experimental cuts which are imposed to remove the J/ψ and ψ' resonant regions are indicated in Fig. 5. The effect of logarithmic QED corrections becomes important for more restrictive cuts on q^2 , and they have been worked out for different choices of the q^2 -range in a recent paper⁴⁹.

3.2. Exclusive Decays $B \rightarrow (K, K^*) \ell^+ \ell^-$

The $B \rightarrow K$ and $B \rightarrow K^*$ transitions involve the following weak currents:

$$\Gamma_\mu^1 = \bar{s} \gamma_\mu (1 - \gamma_5) b, \quad \Gamma_\mu^2 = \bar{s} \sigma_{\mu\nu} q^\nu (1 + \gamma_5) b. \quad (9)$$

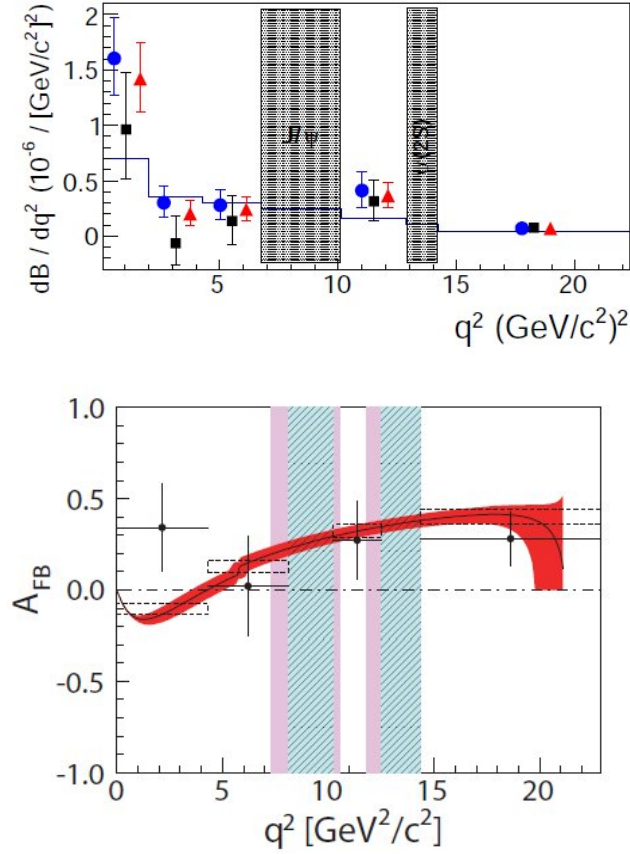


Fig. 5. Dilepton invariant mass Distribution measured by BaBar⁵⁰ (upper frame) and the Forward-backward Asymmetry A_{FB} measured by Belle⁵¹ (lower frame) in $B \rightarrow X_s \ell^+ \ell^-$. The curve (above) and the band (below) are the SM expectations, discussed in the text.

Their matrix elements involve altogether 10 non-perturbative q^2 -dependent functions (form factors), denoted by the following functions:^b

$$\begin{aligned} \langle K | \Gamma_\mu^1 | B \rangle &\supset f_+^K(q^2), f_-^K(q^2). \\ \langle K | \Gamma_\mu^2 | B \rangle &\supset f_T^K(q^2). \\ \langle K^* | \Gamma_\mu^1 | B \rangle &\supset V(q^2), A_1(q^2), A_2(q^2), A_3(q^2). \\ \langle K^* | \Gamma_\mu^2 | B \rangle &\supset T_1(q^2), T_2(q^2), T_3(q^2). \end{aligned}$$

Data on $B \rightarrow K^* \gamma$ provides normalisation of $T_1(0) = T_2(0) \simeq 0.28$. These form factors have been calculated using a number of non-perturbative techniques, in par-

^bAs we will also discuss later the decays $B \rightarrow \pi \ell^+ \ell^-$, we distinguish the $B \rightarrow K$ and $B \rightarrow \pi$ form factors by a superscript.

ticular the QCD sum rules^{12,52} and Lattice QCD^{53,54,56}. They are complementary to each other, as the former are reliable in the low- q^2 domain and the latter can calculate only for large- q^2 . They are usually combined to get reliable profiles of the form factors in the entire q^2 domain. However, heavy quark symmetry allows to reduce the number of independent form factors from 10 to 3 in low- q^2 domain ($q^2/m_b^2 \ll 1$). Symmetry-breaking corrections have been evaluated⁵⁷. The decay rate, dilepton invariant mass distribution and the Forward-backward asymmetry in the low- q^2 region have been calculated for $B \rightarrow K^* \ell^+ \ell^-$ using the SCET formalism⁵⁸. Current measurements of the branching ratios in the inclusive and exclusive semileptonic decays involving $b \rightarrow s$ transition are summarised in Table 2 and compared with the corresponding SM estimates. The inclusive measurements and the SM rates include a cut on the dilepton invariant mass $M_{\ell^+ \ell^-} > 0.2$ GeV. They are in agreement with each other, though precision is currently limited due to the imprecise knowledge of the form factors.

3.3. Current tests of lepton universality in semileptonic B -decays

Currently, a number of measurements in B decays suggests a breakdown of the lepton (e, μ, τ) universality in semileptonic processes. In the SM, gauge bosons couple with equal strength to all three leptons and the couplings of the Higgs to a pair of charged lepton is proportional to the charged lepton mass, which are negligibly small for $\ell^+ \ell^- = e^+ e^-, \mu^+ \mu^-$. Hence, if the lepton non-universality is experimentally established, it would be a fatal blow to the SM.

We briefly summarise the experimental situation starting from the decay $B^\pm \rightarrow K^\pm \ell^+ \ell^-$, whose decay rates were discussed earlier. Theoretical accuracy is vastly improved if instead of the absolute rates, ratios of the decay rates are computed. Data on the decays involving $K^{(*)} \tau^+ \tau^-$ is currently sparse, but first measurements of the ratios involving the final states $K^{(*)} \mu^+ \mu^-$ and $K^{(*)} e^+ e^-$ are available. In particular, a 2.6σ deviation from the e - μ universality is reported by the LHCb collaboration in the ratio involving $B^\pm \rightarrow K^\pm \mu^+ \mu^-$ and $B^\pm \rightarrow K^\pm e^+ e^-$ measured in the low- q^2 region, which can be calculated rather accurately. In the interval $1 \leq q^2 \leq 6$ GeV², LHCb finds⁵⁹

$$R_K \equiv \frac{\Gamma(B^\pm \rightarrow K^\pm \mu^+ \mu^-)}{\Gamma(B^\pm \rightarrow K^\pm e^+ e^-)} = 0.745_{-0.074}^{+0.090}(\text{stat}) \pm 0.035(\text{syst}). \quad (10)$$

This ratio in the SM is close to 1 to a very high accuracy⁶⁰ over the entire q^2 region measured by the LHCb. Thus, the measurement in (10) amounts to about 2.6σ deviation from the SM. Several BSM scenarios have been proposed to account for the R_K anomaly, discussed below, including a Z' -extension of the SM⁶¹. It should, however, be noted that the currently measured branching ratios $\mathcal{B}(B^\pm \rightarrow K^\pm e^+ e^-) = (1.56_{-0.15-0.4}^{+0.19+0.06}) \times 10^{-7}$ and $\mathcal{B}(B^\pm \rightarrow K^\pm \mu^+ \mu^-) = (1.20 \pm 0.09 \pm 0.07) \times 10^{-7}$ are also lower than the SM estimates $\mathcal{B}^{\text{SM}}(B^\pm \rightarrow K^\pm e^+ e^-) = \mathcal{B}^{\text{SM}}(B^\pm \rightarrow K^\pm \mu^+ \mu^-) = (1.75_{-0.29}^{+0.60}) \times 10^{-7}$, and the experimental error on the $\mathcal{B}(B^\pm \rightarrow K^\pm e^+ e^-)$ is twice as

large. One has to also factor in that the electrons radiate very profusely (compared to the muons) and implementing the radiative corrections in hadronic machines is anything but straight forward. In coming years, this and similar ratios, which can also be calculated to high accuracy, will be measured with greatly improved precision at the LHC and Belle II.

The other place where lepton non-universality is reported is in the ratios of the decays $B \rightarrow D^{(*)}\tau\nu_\tau$ and $B \rightarrow D^{(*)}\ell\nu_\ell$. Defining

$$R_{D^{(*)}}^{\tau/\ell} \equiv \frac{\mathcal{B}(B \rightarrow D^{(*)}\tau\nu_\tau)/\mathcal{B}^{\text{SM}}(B \rightarrow D^{(*)}\tau\nu_\tau)}{\mathcal{B}(B \rightarrow D^{(*)}\ell\nu_\ell)/\mathcal{B}^{\text{SM}}(B \rightarrow D^{(*)}\ell\nu_\ell)}, \quad (11)$$

the current averages of the BaBar, Belle, and the LHCb data are²³:

$$R_D^{\tau/\ell} = 1.37 \pm 0.17; \quad R_{D^*}^{\tau/\ell} = 1.28 \pm 0.08. \quad (12)$$

This amounts to about 3.9σ deviation from the τ/ℓ ($\ell = e, \mu$) universality. Interestingly, this happens in a tree-level charged current process. If confirmed experimentally, this would call for a drastic contribution to an effective four-Fermi LL operator $(\bar{c}\gamma_\mu b_L)(\tau_L\gamma_\mu\nu_L)$. It is then conceivable that the non-universality in R_K (which is a loop-induced $b \rightarrow s$ process) is also due to an LL operator $(\bar{s}\gamma_\mu b_L)(\bar{\mu}_L\gamma_\mu\mu_L)$. Several suggestions along these lines involving a leptoquark have been made⁶²⁻⁶⁴. It is worth recalling that leptoquarks were introduced by Pati and Salam in 1973 in an attempt to unify leptons and quarks in $SU(4)$ ^{65,66}. The lepton non-universality in B decays has revived the interest in theories with low-mass leptoquarks, discussed recently in a comprehensive work on this topic⁶⁷.

Table 2. Measurements [PDG 2014] and SM-based estimates⁴⁴ of the branching ratios $\mathcal{B}(B \rightarrow (X_s, K, K^*)\ell^+\ell^-)$ in units of 10^{-6}

Decay Mode	Expt. (BELLE & BABAR)	Theory (SM)
$B \rightarrow K\ell^+\ell^-$	0.48 ± 0.04	0.35 ± 0.12
$B \rightarrow K^*e^+e^-$	1.19 ± 0.20	1.58 ± 0.49
$B \rightarrow K^*\mu^+\mu^-$	1.06 ± 0.09	1.19 ± 0.39
$B \rightarrow X_s\mu^+\mu^-$	4.3 ± 1.2	4.2 ± 0.7
$B \rightarrow X_se^+e^-$	4.7 ± 1.3	4.2 ± 0.7
$B \rightarrow X_s\ell^+\ell^-$	4.5 ± 1.0	4.2 ± 0.7

3.4. Angular analysis of the decay $B^0 \rightarrow K^{*0}(\rightarrow K^+\pi^-)\mu^+\mu^-$

For the inclusive decays $B \rightarrow X_s \ell^+ \ell^-$, the observables which have been measured are the integrated rates, the dilepton invariant mass $d\Gamma/dq^2$ and the FB asymmetry $A_{\text{FB}}(q^2)$. They are all found to be in agreement with the SM. In the exclusive decays such as $B \rightarrow K^* \ell^+ \ell^-$ and $B_s \rightarrow \phi \ell^+ \ell^-$, a complete angular analysis of the decay is experimentally feasible. This allows one to measure a number of additional observables, defined below.

$$\begin{aligned} \frac{1}{d(\Gamma + \bar{\Gamma})} \frac{d^4(\Gamma + \bar{\Gamma})}{dq^2 d\Omega} = & \frac{9}{32\pi} \left[\frac{3}{4}(1 - F_L) \sin^2 \theta_K + F_L \cos^2 \theta_K \right. \\ & + \frac{1}{4}(1 - F_L) \sin^2 \theta_K \cos 2\theta_\ell - F_L \cos^2 \theta_K \cos 2\theta_\ell \\ & + S_3 \sin^2 \theta_K \sin^2 \theta_\ell \cos 2\phi + S_4 \sin 2\theta_K \sin 2\theta_\ell \cos \phi \\ & + S_5 \sin 2\theta_K \sin \theta_\ell \cos \phi + \frac{4}{3} A_{\text{FB}} \sin^2 \theta_K \cos \theta_\ell \\ & + S_7 \sin 2\theta_K \sin \theta_\ell \sin \phi + S_8 \sin 2\theta_K \sin 2\theta_\ell \sin \phi \\ & \left. + S_9 \sin^2 \theta_K \sin^2 \theta_\ell \sin 2\phi \right]. \end{aligned} \quad (13)$$

The three angles θ_K , θ_ℓ and ϕ for the decay $B^0 \rightarrow K^{*0}(\rightarrow K^+\pi^-)\mu^+\mu^-$ are defined in Fig. 6. An angular analysis of the decay chains $B^0 \rightarrow K^{*0}(\rightarrow K^+\pi^-)\mu^+\mu^-$ ⁶⁸

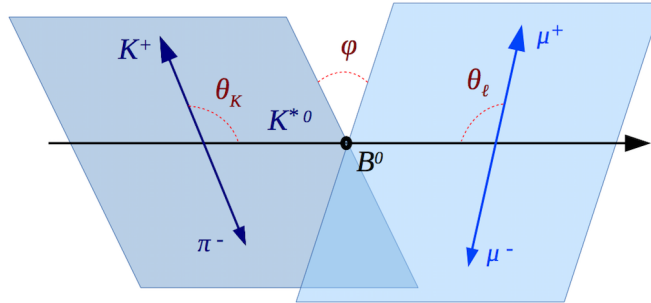


Fig. 6. Definitions of the angles in $B^0 \rightarrow K^{*0}(\rightarrow K^+\pi^-)\mu^+\mu^-$.

and $B_s^0 \rightarrow \phi(\rightarrow K^+K^-)\mu^+\mu^-$ ⁶⁹ has been carried out by LHCb.

The observables in (13) are q^2 -dependent coefficients of the Wilson coefficients and hence they probe the underlying dynamics. Since these coefficients have been calculated to a high accuracy, the remaining theoretical uncertainty lies in the form factors and also from the charm-quark loops. The form factors have been calculated using the QCD sum rules and in the high- q^2 region also using lattice QCD. They limit the current theoretical accuracy. However, a number of so-called optimised observables has been proposed⁷⁰, which reduce the dependence on the form factors.

Using the LHCb convention, these observables are defined as⁶⁸

$$P_1 \equiv 2S_3/(1 - F_L); \quad P_2 \equiv 2A_{\text{FB}}/3(1 - F_L); \quad P_3 \equiv -S_9/(1 - F_L),$$

$$P'_{4,5,6,8} \equiv S_{4,5,7,8}/\sqrt{F_L(1 - F_L)}. \quad (14)$$

These angular observables have been analysed in a number of theoretical stud-

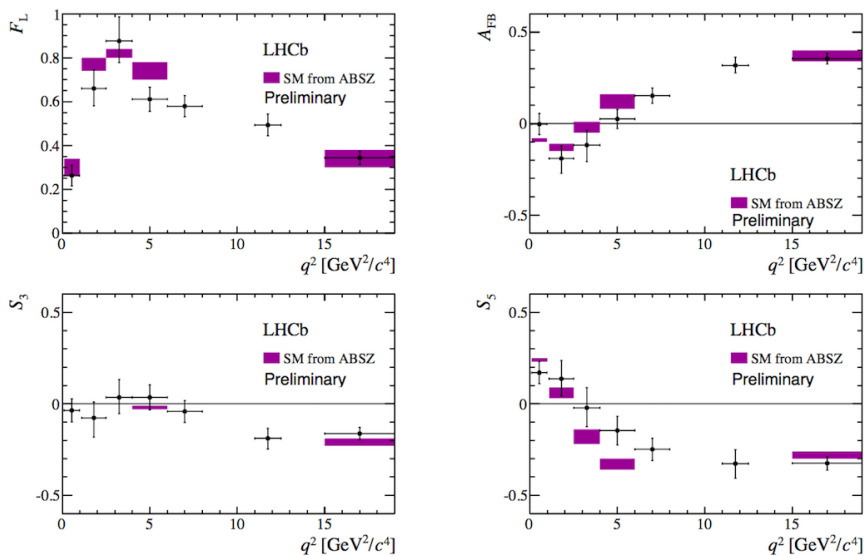


Fig. 7. CP-averaged variables in bins of q^2 for the observables F_L , A_{FB} , S_3 and S_5 in $B^0 \rightarrow K^{*0}(\rightarrow K^+\pi^-)\mu^+\mu^-$ measured by LHCb⁶⁸ and comparison with the SM⁷³.

ies^{13,71–75}, which differ in the treatment of their non-perturbative input, mainly form factors. The LHCb collaboration, which currently dominates this field, has used these SM-based estimates and compared with their data in various q^2 bins. Two representative comparisons based on the theoretical estimates from Altmannshofer and Straub⁷³ and Descotes-Genon, Hofer, Matias and Virto⁷⁵ are shown in Figs. 7 and 8, respectively. They are largely in agreement with the data, except for the distributions in the observables $S_5(q^2)$ (in Fig. 7) and $P'_5(q^2)$ (in Fig. 8) in the bins around $q^2 \geq 5$ GeV². The pull on the SM depends on the theoretical model, reaching 3.4σ in the bin $4.3 \leq q^2 \leq 8.68$ GeV² compared to DHMV⁷⁵. There are deviations of a similar nature, between 2 and 3σ , seen in the comparison of S_5 and other quantities, such as the partial branching ratios in $B \rightarrow K^*\mu^+\mu^-$, $B_s \rightarrow \phi\mu^+\mu^-$ and $F_L(q^2)$ ⁷³.

An analysis of the current Belle data⁷⁶, shown in Fig. 9, displays a similar pattern as the one reported by LHCb. As the Belle data has larger errors, due to limited statistics, the resulting pull on the SM is less significant. In the interval $4.0 \leq q^2 \leq 8.0$ GeV², Belle reports deviations of 2.3σ (compared to DHMV⁷⁵),

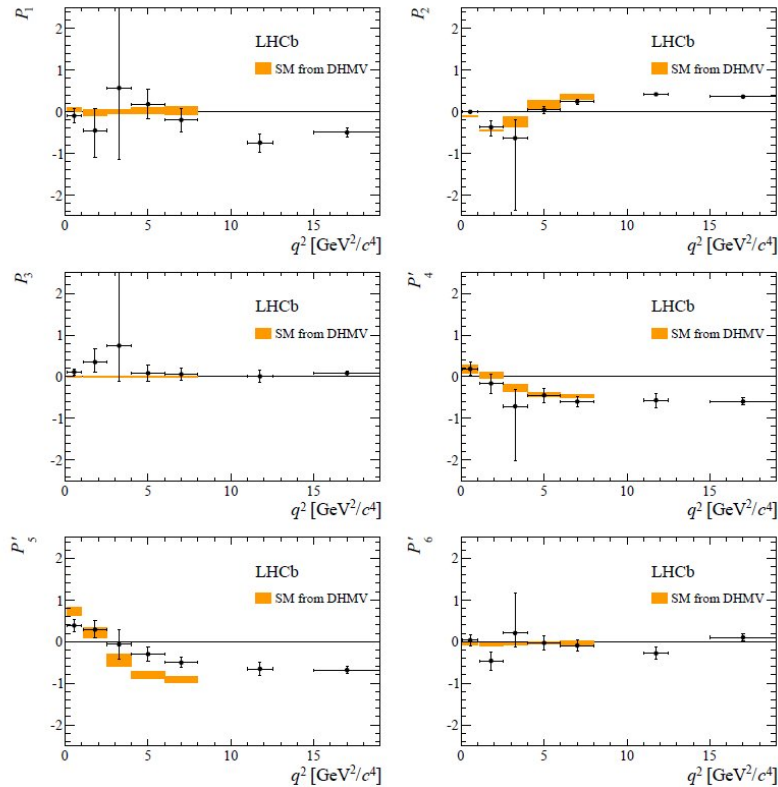


Fig. 8. The optimised angular observables in bins of q^2 in the decay $B^0 \rightarrow K^{*0}(\rightarrow K^+\pi^-)\mu^+\mu^-$ measured by the LHCb collaboration⁶⁸ and comparison with the SM⁷⁵.

1.72σ (compared to BSZ¹³) and 1.68σ (compared to JC⁷²). These measurements will improve greatly at Belle II.

To quantify the deviation of the LHCb data from the SM estimates, a $\Delta\chi^2$ distribution for the real part of the Wilson coefficient $\text{Re}C_9(m_b)$ is shown in Fig. 10. In calculating the $\Delta\chi^2$, the other Wilson coefficients are set to their SM values. The coefficient $\text{Re}C_9^{\text{SM}}(m_b) = 4.27$ at the NNLO accuracy in the SM is indicated by a vertical line. The best fit of the LHCb data yields a value which is shifted from the SM, and the deviation in this coefficient is found to be $\Delta\text{Re}C_9(m_b) = -1.04 \pm 0.25$. The deviation is tantalising, but not yet conclusive. A bit of caution is needed here as the SM estimates used in the analysis above may have to be revised, once the residual uncertainties are better constrained. In particular, the hadronic contributions generated by the four-quark operators with charm are difficult to estimate, especially around $q^2 \sim 4m_c^2$, leading to an effective shift in the value of the Wilson coefficient being discussed⁷⁷.

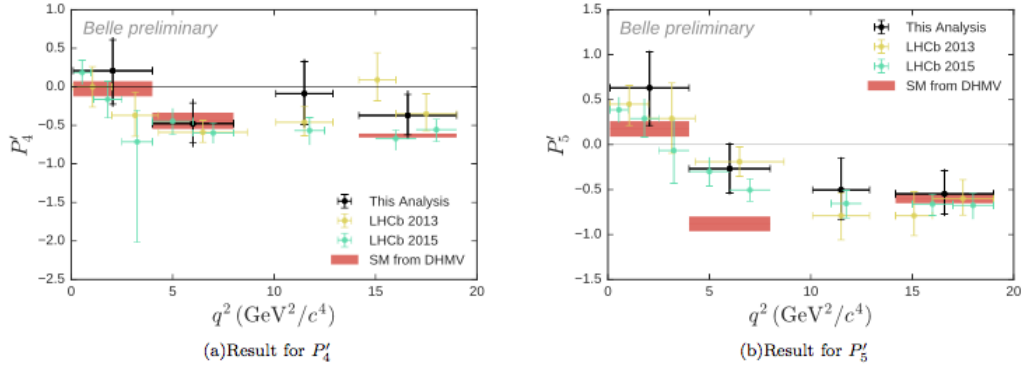


Fig. 9. The optimised angular observables P'_4 and P'_5 in bins of q^2 in the decay $B^0 \rightarrow K^{*0}(\rightarrow K^+\pi^-)\mu^+\mu^-$ measured by Belle⁷⁶ and comparison with the SM⁷⁵.

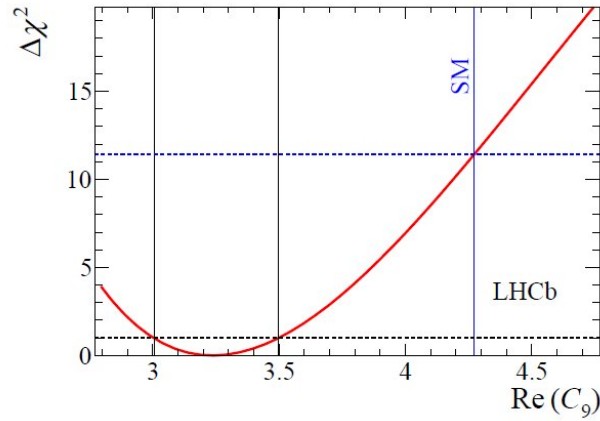


Fig. 10. The $\Delta\chi^2$ distribution for the real part of the Wilson coefficient $\text{Re}C_9(m_b)$ from a fit of the CP-averaged observables $F_L, A_{\text{FB}}, S_3, \dots, S_9$ in $B^0 \rightarrow K^{*0}(\rightarrow K^+\pi^-)\mu^+\mu^-$ by the LHCb collaboration⁶⁸.

4. CKM-suppressed $b \rightarrow d\ell^+\ell^-$ transitions in the SM

Weak transitions $b \rightarrow d\ell^+\ell^-$, like the radiative decays $b \rightarrow d\gamma$, are CKM suppressed and because of this the structure of the effective weak Hamiltonian is different than the one encountered earlier for the $b \rightarrow s\ell^+\ell^-$ transitions.

$$\mathcal{H}_{\text{eff}}^{b \rightarrow d} = -\frac{4G_F}{\sqrt{2}} \left[V_{tb}^* V_{td} \sum_{i=1}^{10} C_i(\mu) (O_i(\mu) + V_{ub}^* V_{ud} \sum_{i=1}^2 C_i(\mu) (O_i(\mu) - O_i(\mu))) \right] + \text{h.c.} \quad (15)$$

Here $O_i(\mu)$ are the dimension-six operators introduced earlier (except for the interchange $s \rightarrow d$ quark) in $\mathcal{H}_{\text{eff}}^{b \rightarrow s}$. As the two CKM factors are comparable in magnitude $|V_{tb}^* V_{td}| \simeq |V_{ub}^* V_{ud}|$, and have different weak phases, we anticipate sizeable CP-violating asymmetries in both the inclusive $b \rightarrow d\ell^+\ell^-$ and exclusive transitions, such as $B \rightarrow (\pi, \rho)\ell^+\ell^-$. The relevant operators appearing in $\mathcal{H}_{\text{eff}}^{b \rightarrow d}$ are:

Tree operators

$$\mathcal{O}_1 = (\bar{d}_L \gamma_\mu T^A c_L) (\bar{c}_L \gamma^\mu T^A b_L), \quad \mathcal{O}_2 = (\bar{d}_L \gamma_\mu c_L) (\bar{c}_L \gamma^\mu b_L), \quad (16)$$

$$\mathcal{O}_1^{(u)} = (\bar{d}_L \gamma_\mu T^A u_L) (\bar{u}_L \gamma^\mu T^A b_L), \quad \mathcal{O}_2^{(u)} = (\bar{d}_L \gamma_\mu u_L) (\bar{u}_L \gamma^\mu b_L). \quad (17)$$

Dipole operators

$$\mathcal{O}_7 = \frac{e m_b}{g_s^2} (\bar{d}_L \sigma^{\mu\nu} b_R) F_{\mu\nu}, \quad \mathcal{O}_8 = \frac{m_b}{g_s} (\bar{d}_L \sigma^{\mu\nu} T^A b_R) G_{\mu\nu}^A. \quad (18)$$

Semileptonic operators

$$\mathcal{O}_9 = \frac{e^2}{g_s^2} (\bar{d}_L \gamma^\mu b_L) \sum_\ell (\bar{\ell} \gamma_\mu \ell), \quad \mathcal{O}_{10} = \frac{e^2}{g_s^2} (\bar{d}_L \gamma^\mu b_L) \sum_\ell (\bar{\ell} \gamma_\mu \gamma_5 \ell). \quad (19)$$

Here, $e(g_s)$ is the QED (QCD) coupling constant. Since the inclusive decay $B \rightarrow X_d \ell^+\ell^-$ has not yet been measured, but hopefully will be at Belle II, we discuss the exclusive decay $B^+ \rightarrow \pi^+ \ell^+\ell^-$, which is the only $b \rightarrow d$ semileptonic transition measured so far.

4.1. Exclusive decay $B^+ \rightarrow \pi^+ \ell^+\ell^-$

The decay $B^+ \rightarrow \pi^+ \ell^+\ell^-$ is induced by the vector and tensor currents and their matrix elements are defined as

$$\langle \pi(p_\pi) | \bar{b} \gamma^\mu d | B(p_B) \rangle = f_+^\pi(q^2) (p_B^\mu + p_\pi^\mu) + [f_0^\pi(q^2) - f_+^\pi(q^2)] \frac{m_B^2 - m_\pi^2}{q^2} q^\mu, \quad (20)$$

$$\langle \pi(p_\pi) | \bar{b} \sigma^{\mu\nu} q_\nu d | B(p_B) \rangle = \frac{i f_T^\pi(q^2)}{m_B + m_\pi} [(p_B^\mu + p_\pi^\mu) q^2 - q^\mu (m_B^2 - m_\pi^2)]. \quad (21)$$

These form factors are related to the ones in the decay $B \rightarrow K \ell^+\ell^-$, called $f_i^K(q^2)$, discussed earlier, by $SU(3)_F$ symmetry. Of these, the form factors $f_+^\pi(q^2)$ and $f_0^\pi(q^2)$ are related by isospin symmetry to the corresponding ones measured in the charged current process $B^0 \rightarrow \pi^- \ell^+ \nu_\ell$ by Babar and Belle, and they can be extracted from the data. This has been done using several parameterisations of the form factors with all of them giving an adequate description of the data⁷⁸. Due to their analytic properties, the so-called z -expansion methods, in which the form factors are expanded in a Taylor series in z , employed in the Boyd-Grinstein-Lebed

^cCharge conjugation is implied here.

(BGL) parametrisation⁷⁹ and the Bourrely-Caprini-Lellouch (BCL)⁸⁰ parametrisation, are preferable.

The BGL parametrisation is used in working out the decay rate and the invariant dilepton mass distribution⁷⁸ for $B^+ \rightarrow \pi^+ \ell^+ \ell^-$, which is discussed below. The BCL-parametrisation is used by the lattice-QCD groups, the HPQCD^{54,55} and Fermilab/MILC⁵⁶ collaborations, to determine the form factors $f_i^\pi(q^2)$ and $f_i^K(q^2)$. In particular, the Fermilab/MILC collaboration has worked out the dilepton invariant mass distribution in the decay of interest $B^+ \rightarrow \pi^+ \ell^+ \ell^-$, making use of their simulation in the large- q^2 region and extrapolating with the BCL parametrisation.

We first discuss the low- q^2 region ($q^2 \ll m_b^2$). In this case, heavy quark symmetry (HQS) relates all three form factors of interest $f_i^\pi(q^2)$ and this can be used advantageously to have a reliable estimate of the dilepton invariant mass spectrum in this region. Including lowest order HQS-breaking, the resulting expressions for the form factors (for $q^2/m_b^2 \ll 1$) are worked out by Beneke and Feldmann⁵⁷. Thus, fitting the form factor $f_+(q^2)$ from the charged current data on $B \rightarrow \pi \ell^+ \nu_\ell$ decay, and taking into account the HQS and its breaking, lead to a model-independent predictions of the differential branching ratio (dimuon mass spectrum) in the neutral current process $B^+ \rightarrow \pi^+ \ell^+ \ell^-$ for low- q^2 values. However, the long-distance contribution, which arises from the processes $B^+ \rightarrow \pi^+(\rho^0, \omega) \rightarrow \pi^+ \mu^+ \mu^-$ are not included here. The SM invariant dilepton mass distribution in $B^+ \rightarrow \pi^+ \ell^+ \ell^-$ integrated over the range $1\text{GeV}^2 \leq q^2 \leq 8\text{GeV}^2$ yields a partial branching ratio

$$\mathcal{B}(B^+ \rightarrow \pi^+ \mu^+ \mu^-) = (0.57_{-0.05}^{+0.07}) \times 10^{-8}. \quad (22)$$

Thanks to the available data on the charged current process and heavy quark symmetry, this enables an accuracy of about 10% for an exclusive branching ratio, comparable to the theoretical accuracy in the inclusive decay $B \rightarrow X_s \gamma$, discussed earlier. Thus, the decay $B^+ \rightarrow \pi^+ \mu^+ \mu^-$ offers a key advantage compared to the decay $B^+ \rightarrow K^+ \ell^+ \ell^-$, in which case the charged current process is not available.

The differential branching ratio in the entire q^2 region is given by

$$\frac{d\mathcal{B}(B^+ \rightarrow \pi^+ \ell^+ \ell^-)}{dq^2} = C_B |V_{tb} V_{td}^*|^2 \sqrt{\lambda(q^2)} \sqrt{1 - \frac{4m_\ell^2}{q^2}} F(q^2), \quad (23)$$

where the constant $C_B = G_F^2 \alpha_{\text{em}}^2 \tau_B / 1024 \pi^5 m_B^3$ and $\lambda(q^2)$ is the usual kinematic function $\lambda(q^2) = (m_B^2 + m_\pi^2 - q^2)^2 - 4m_B^2 m_\pi^2$. The function $F(q^2)$ depends on the effective Wilson coefficients, C_7^{eff} , C_9^{eff} , and C_{10}^{eff} , and the three form factors $f_+^\pi(q^2)$, $f_0^\pi(q^2)$ and $f_T^\pi(q^2)$. A detailed discussion of the determination of the form factors, of which only $f_+^\pi(q^2)$ and $f_T^\pi(q^2)$ are numerically important for $\ell^\pm = e^\pm, \mu^\pm$ is given elsewhere⁷⁸. We recall that $f_+^\pi(q^2)$ is constrained by the data on the charged current process in the entire q^2 domain. In addition, the lattice-QCD results on the form factors in the large- q^2 domain and the HQS-based relations in the low- q^2 region provide sufficient constraints on the form factor. This has enabled a rather precise determination of the invariant dilepton mass distribution in $B^+ \rightarrow \pi^+ \ell^+ \ell^-$.

Taking into account the various parametric and form-factor dependent uncertainties, this yields the following estimate for the branching ratio for $B^+ \rightarrow \pi^+ \mu^+ \mu^-$ ⁸²

$$\mathcal{B}_{\text{SM}}(B^+ \rightarrow \pi^+ \mu^+ \mu^-) = (1.88_{-0.21}^{+0.32}) \times 10^{-8}, \quad (24)$$

to be compared with the measured branching ratio by the LHCb collaboration⁸² (based on 3fb^{-1} data):

$$\mathcal{B}_{\text{LHCb}}(B^+ \rightarrow \pi^+ \mu^+ \mu^-) = (1.83 \pm 0.24 \pm 0.05) \times 10^{-8}, \quad (25)$$

where the first error is statistical and the second systematic, resulting in excellent agreement. The dimuon invariant mass distribution measured by the LHCb collaboration⁸² is shown in Fig. 11, and compared with the SM-based theoretical prediction, called APR13⁷⁸, and the lattice-based calculation, called FNAL/MILC 15⁵⁶. Also shown is a comparison with a calculation, called HKR⁸¹, which has essentially the same short-distance contribution in the low- q^2 region, as discussed earlier, but additionally takes into account the contributions from the lower resonances ρ, ω and ϕ . This adequately describes the distribution in the q^2 bin, around 1 GeV^2 .

With the steadily improving lattice calculations for the various input hadronic quantities and the form factors, theoretical error indicated in Eq. (24) will go down considerably. Experimentally, we expect rapid progress due to the increased statistics at the LHC, but also from Belle II, which will measure the corresponding distributions and branching ratio also in the decays $B^+ \rightarrow \pi^+ e^+ e^-$, and $B^+ \rightarrow \pi^+ \tau^+ \tau^-$, providing a complementary test of the $e\text{-}\mu\text{-}\tau$ universality in $b \rightarrow d$ semileptonic transitions.

5. Leptonic Rare B Decays

The final topic discussed in this write-up involves purely leptonic decays $B_s^0 \rightarrow \ell^+ \ell^-$ and $B^0 \rightarrow \ell^+ \ell^-$ with $\ell^+ \ell^- = e^+ e^-, \mu^+ \mu^-, \tau^+ \tau^-$. Of these, $\mathcal{B}(B_s^0 \rightarrow \mu^+ \mu^-) = (2.8_{-0.6}^{+0.7}) \times 10^{-9}$ is now well measured, and the corresponding CKM-suppressed decay $\mathcal{B}(B^0 \rightarrow \mu^+ \mu^-) = (3.9_{-1.4}^{+1.6}) \times 10^{-10}$ is almost on the verge of becoming a measurement. These numbers are from the combined CMS/LHCb data⁸³. From the experimental point of view, their measurement is a real *tour de force*, considering the tiny branching ratios and the formidable background at the LHC.

In the SM, these decays are dominated by the axial-vector operator $O_{10} = (\bar{s}_\alpha \gamma^\mu P_L b_\alpha)(\bar{\ell} \gamma_\mu \gamma_5 \ell)$. In principle, the operators $O_S = m_b(\bar{s}_\alpha \gamma^\mu P_R b_\alpha)(\bar{\ell} \ell)$ and $O_P = m_b(\bar{s}_\alpha \gamma^\mu P_R b_\alpha)(\bar{\ell} \gamma_5 \ell)$ also contribute, but are chirally suppressed in the SM. This need not be the case in BSM scenarios, and hence the great interest in measuring these decays precisely. In the SM, the measurement of $\mathcal{B}(B_s^0 \rightarrow \mu^+ \mu^-)$ and $\mathcal{B}(B^0 \rightarrow \mu^+ \mu^-)$ provide a measurement of the Wilson coefficient $C_{10}(m_b)$. Their ratio $\mathcal{B}(B^0 \rightarrow \mu^+ \mu^-)/\mathcal{B}(B_s^0 \rightarrow \mu^+ \mu^-)$ being proportional to the ratio of the CKM matrix-elements $|V_{td}/V_{ts}|^2$ is an important constraint on the CKM unitarity triangle.

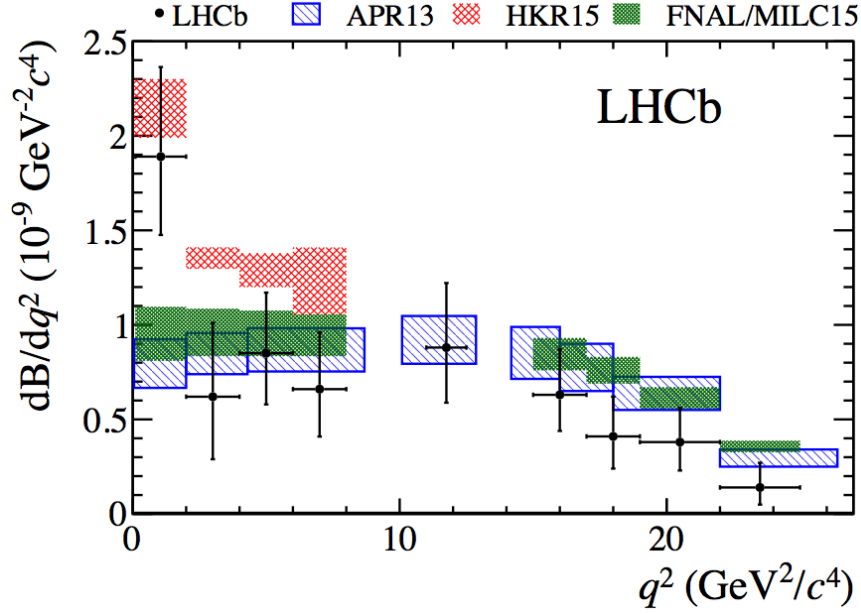


Fig. 11. Comparison of the dimuon invariant mass distribution in $B^+ \rightarrow \pi^+ \mu^+ \mu^-$ in the SM with the LHCb data⁸². Theoretical distributions shown are : APR13⁷⁸, HKR15⁸¹, and FNAL/MILC⁵⁶.

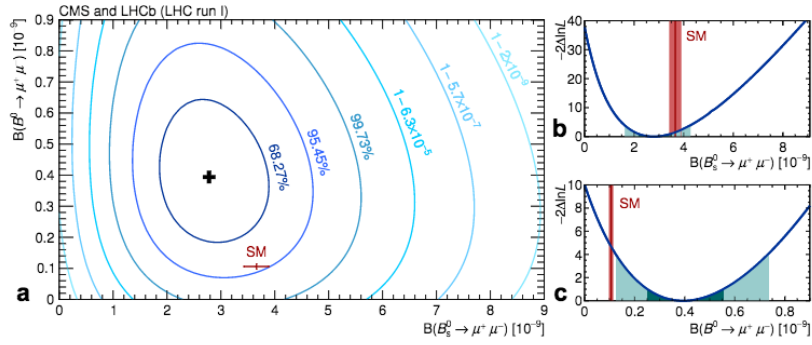


Fig. 12. Likelihood contours in the $\mathcal{B}(B^0 \rightarrow \mu^+ \mu^-)$ versus $\mathcal{B}(B_s^0 \rightarrow \mu^+ \mu^-)$ plane. The (black) cross in (a) marks the best-fit value and the SM expectation is shown as the (red) marker. Variations of the test statistics $-2\Delta \ln L$ for $\mathcal{B}(B_s^0 \rightarrow \mu^+ \mu^-)$ (b) and $\mathcal{B}(B^0 \rightarrow \mu^+ \mu^-)$ (c) are shown. The SM prediction is denoted with the vertical (red) bars. (From the combined CMS-LHCb data⁸³.)

The decay rate $\Gamma(B_s^0 \rightarrow \mu^+ \mu^-)$ in the SM can be written as

$$\Gamma(B_s^0 \rightarrow \mu^+ \mu^-) = \frac{G_F^2 M_W^2 m_{B_s}^3 f_{B_s}^2}{8\pi^5} |V_{tb}^* V_{ts}|^2 \frac{4m_\ell^2}{m_{B_s}^2} \sqrt{1 - \frac{4m_\ell^2}{m_{B_s}^2}} |C_{10}|^2 + O(\alpha_{\text{em}}). \quad (26)$$

The coefficient C_{10} has been calculated by taking into account the NNLO QCD corrections and NLO electroweak corrections, but the $O(\alpha_{\text{em}})$ contribution indicated above is ignored, as it is small. The SM branching ratio in this accuracy have been obtained in⁸⁴⁻⁸⁶, where a careful account of the various input quantities is presented. The importance of including the effects of the width difference $\Delta\Gamma_s$ due to the $B_s^0 - \bar{B}_s^0$ mixings in extracting the branching ratio for $B_s \rightarrow \mu^+\mu^-$ has been emphasised in the literature⁸⁷ and is included in the analysis. The time-averaged branching ratios, which in the SM to a good approximation equals to $\bar{\mathcal{B}}(B_s \rightarrow \mu^+\mu^-) = \Gamma(B_s \rightarrow \mu^+\mu^-)/\Gamma_H(B_s)$, where $\Gamma_H(B_s)$ is the heavier mass-eigenstate total width, is given below⁸⁴

$$\bar{\mathcal{B}}(B_s \rightarrow \mu^+\mu^-) = (3.65 \pm 0.23) \times 10^{-9}. \quad (27)$$

In evaluating this, a value $f_{B_s} = 227.7(4.5)$ MeV was used from the earlier FLAG average⁸⁸. In the most recent compilation by the FLAG collaboration⁹, this coupling constant has been updated to $f_{B_s} = 224(5)$ MeV, which reduces the branching ratio to $\bar{\mathcal{B}}(B_s \rightarrow \mu^+\mu^-) = (3.55 \pm 0.23) \times 10^{-9}$. This is compatible with the current measurements to about 1σ , with the uncertainty dominated by the experiment.

The corresponding branching ratio $\bar{\mathcal{B}}(B^0 \rightarrow \mu^+\mu^-)$ is evaluated as⁸⁴

$$\bar{\mathcal{B}}(B^0 \rightarrow \mu^+\mu^-) = (1.06 \pm 0.09) \times 10^{-10}, \quad (28)$$

which, likewise, has to be scaled down to $(1.01 \pm 0.09) \times 10^{-10}$, due to the current average⁹ $f_B = 186(4)$ MeV, compared to $f_B = 190.5(4.2)$ MeV used in deriving the result given in Eq. (28). This is about 2σ below the current measurement, and the ratio of the two leptonic decays $\bar{\mathcal{B}}(B_s \rightarrow \mu^+\mu^-)/\bar{\mathcal{B}}(B^0 \rightarrow \mu^+\mu^-)$ is off by about 2.3σ . The likelihood contours in the $\mathcal{B}(B^0 \rightarrow \mu^+\mu^-)$ versus $\mathcal{B}(B_s^0 \rightarrow \mu^+\mu^-)$ plane from the combined CMS/LHCb data are shown in Fig. 12.

The anomalies in the decays $B \rightarrow K^*\mu^+\mu^-$, discussed previously, and the deviations in $\mathcal{B}(B^0 \rightarrow \mu^+\mu^-)$ and $\mathcal{B}(B_s^0 \rightarrow \mu^+\mu^-)$, if consolidated experimentally, would require an extension of the SM. A recent proposal based on the group $SU(3)_C \times SU(3)_L \times U(1)$ is discussed by Buras, De Fazio and Girrbach⁸⁹. Lepton non-universality, if confirmed, requires a leptoquark-type solution. A viable candidate theory to replace the SM and accounting for all the current anomalies, in my opinion, is not in sight.

6. Global fits of the Wilson Coefficients C_9 and C_{10}

As discussed in the foregoing, a number of deviations from the SM-estimates are currently present in the data on semileptonic and leptonic rare B -decays. They lie mostly around 2 to 3σ . A comparison of the LHCb data on a number of angular observables $F_L, A_{\text{FB}}, S_3, \dots, S_9$ in $B^0 \rightarrow K^{*0}(\rightarrow K^+\pi^-)\mu^+\mu^-$ with the SM-based estimates was shown in Fig. 10, yielding a value of $\text{Re}(C_9)$ which deviates from the SM by about 3σ . A number of groups has undertaken similar fits of the data and the outcome depends on a number of assumed correlations. However, it should be

stressed that there are still non-perturbative contributions present in the current theoretical estimates which are not yet under complete quantitative control. The contributions from the charm quarks in the loops is a case in point. Also, form factor uncertainties are probably larger than assumed in some of these global fits.

As a representative example of the kind of constraints on the Wilson coefficients C_9 and C_{10} that follow from the data on semileptonic and leptonic decays of the B mesons is shown in Fig. 13 from the Fermilab/MILC collaboration⁵⁶. This shows that the SM point indicated by $(0, 0)$ in the $\text{Re}(C_9^{\text{NP}}, \text{Re}(C_{10}^{\text{NP}}))$ -plane lies a little beyond 2σ . In some other fits, the deviations are larger but still far short for a discovery of BSM effects. As a lot of the experimental input in this and similar analysis is due to the LHCb data, this has to be confirmed by an independent experiment. This, hopefully, will be done by Belle II. We are better advised to wait and see if these deviations become statistically significant enough to warrant new physics. Currently, the situation is tantalising but not conclusive.

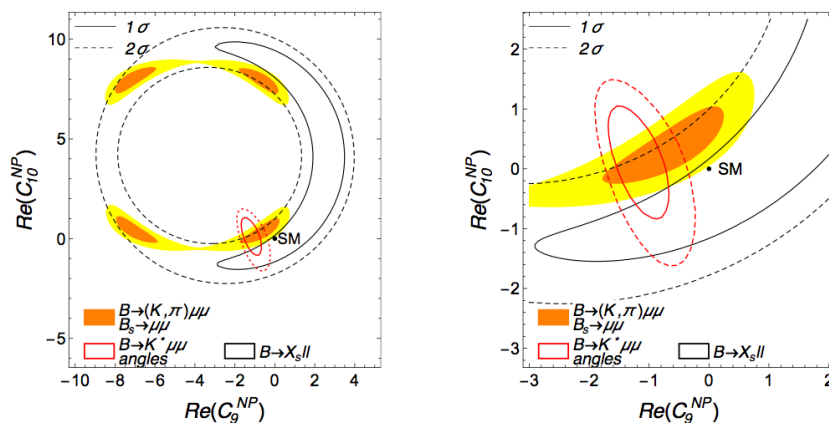


Fig. 13. Present constraints on the Wilson coefficients $\text{Re}C_{10}^{\text{NP}}$ vs. $\text{Re}C_9^{\text{NP}}$ from the semileptonic rare B -decays and $B_s \rightarrow \mu^+ \mu^-$. The SM-point is indicated. (From Fermilab/MILC Lattice Collaboration⁵⁶.)

7. Concluding Remarks

From the measurement by the CLEO collaboration of the rare decay $B \rightarrow X_s \gamma$ in 1995, having a branching ratio of about 3×10^{-4} , to the rarest of the measured B decays, $B^0 \rightarrow \mu^+ \mu^-$, with a branching fraction of about 1×10^{-10} by the LHCb and CMS collaborations, SM has been tested over six orders of magnitude. This is an impressive feat, made possible by dedicated experimental programmes carried out with diverse beams and detection techniques over a period of more than 20 years. A sustained theoretical effort has accompanied the experiments all along, underscoring both the continued theoretical interest in b physics and an intense exchange between

the two communities. With the exception of a few anomalies, showing deviations from the SM ranging between 2 to 4σ in statistical significance, a vast majority of the measurements is in quantitative agreement with the SM. In particular, all quark flavour transitions are described by the CKM matrix whose elements are now determined. The CP asymmetry measured so far in laboratory experiments is explained by the Kobayashi-Maskawa phase. FCNC processes, of which rare B -decays discussed here is a class, are governed by the GIM mechanism, with the particles in the SM (three families of quarks and leptons, electroweak gauge bosons, gluons, and the Higgs) accounting for all the observed phenomena - so far. Whether this astounding consistence will continue will be tested in the coming years, as the LHC experiments analyse more data, enabling vastly improved precision in some of the key measurements discussed here. In a couple of years from now, Belle II will start taking data, providing independent and new measurements. They will be decisive in either deepening our knowledge about the SM, or hopefully in discovering the new frontier of physics.

8. Acknowledgment

I thank Harald Fritzsch for inviting me to this very stimulating conference and Prof. K.K. Phua for the warm hospitality in Singapore. I also thank Mikolaj Misiak for reading the manuscript and helpful suggestions.

References

1. S. L. Glashow, Nucl. Phys. **22**, 579 (1961); S. Weinberg, Phys. Rev. Lett. **19**, 1264 (1967); A. Salam, Conf. Proc. C **680519**, 367 (1968).
2. S. L. Glashow, J. Iliopoulos and L. Maiani, Phys. Rev. D **2**, 1285 (1970).
3. N. Cabibbo, Phys. Rev. Lett. **10**, 531 (1963). M. Kobayashi and T. Maskawa, Prog. Theor. Phys. **49**, 652 (1973).
4. K. A. Olive *et al.* [Particle Data Group Collaboration], Chin. Phys. C **38**, 090001 (2014).
5. A. V. Manohar and M. B. Wise, Camb. Monogr. Part. Phys. Nucl. Phys. Cosmol. **10**, 1 (2000).
6. C. W. Bauer, S. Fleming, D. Pirjol and I. W. Stewart, Phys. Rev. D **63**, 114020 (2001) [hep-ph/0011336]; C. W. Bauer, S. Fleming and M. E. Luke, Phys. Rev. D **63**, 014006 (2000) [hep-ph/0005275]; C. W. Bauer, D. Pirjol and I. W. Stewart, Phys. Rev. D **65**, 054022 (2002) [hep-ph/0109045].
7. M. Beneke, A. P. Chapovsky, M. Diehl and T. Feldmann, Nucl. Phys. B **643**, 431 (2002) [hep-ph/0206152].
8. For an excellent review on SCET and applications, see T. Becher, A. Broggio and A. Ferroglia, Lect. Notes Phys. **896** (2015) [arXiv:1410.1892 [hep-ph]].
9. S. Aoki *et al.*, arXiv:1607.00299 [hep-lat].
10. A. Ali, V. M. Braun and H. Simma, Z. Phys. C **63**, 437 (1994) [hep-ph/9401277].
11. P. Colangelo and A. Khodjamirian, In *Shifman, M. (ed.): At the frontier of particle physics, vol. 3* 1495-1576 [hep-ph/0010175].
12. P. Ball and R. Zwicky, Phys. Rev. D **71**, 014015 (2005) [hep-ph/0406232].
13. A. Bharucha, D. M. Straub and R. Zwicky, arXiv:1503.05534 [hep-ph].

14. R. Ammar *et al.* [CLEO Collaboration], Phys. Rev. Lett. **71**, 674 (1993).
15. M. S. Alam *et al.* [CLEO Collaboration], Phys. Rev. Lett. **74**, 2885 (1995).
16. A. Ali and C. Greub, Phys. Lett. B **259**, 182 (1991); Z. Phys. C **49**, 431 (1991).
17. S. Chen *et al.* [CLEO Collaboration], Phys. Rev. Lett. **87**, 251807 (2001) [hep-ex/0108032].
18. P. Koppenburg *et al.* [Belle Collaboration], Phys. Rev. Lett. **93**, 061803 (2004) [hep-ex/0403004].
19. T. Blake, G. Lanfranchi and D. M. Straub, arXiv:1606.00916 [hep-ph].
20. S. Descotes-Genon, L. Hofer, J. Matias and J. Virto, JHEP **1606**, 092 (2016) [arXiv:1510.04239 [hep-ph]].
21. P. Koppenburg, Z. Dolezal and M. Smizanska, Scholarpedia **11**, 32643 (2016) [arXiv:1606.00999 [hep-ex]].
22. The physics of the B factories is excellently reviewed in A. J. Bevan *et al.* [BaBar and Belle Collaborations], Eur. Phys. J. C **74**, 3026 (2014) [arXiv:1406.6311 [hep-ex]].
23. Y. Amhis *et al.* [Heavy Flavor Averaging Group (HFAG) Collaboration], arXiv:1412.7515 [hep-ex].
24. M. Misiak *et al.*, Phys. Rev. Lett. **114**, no. 22, 221801 (2015) [arXiv:1503.01789 [hep-ph]].
25. M. Czakon, P. Fiedler, T. Huber, M. Misiak, T. Schutzmeier and M. Steinhauser, JHEP **1504**, 168 (2015) [arXiv:1503.01791 [hep-ph]].
26. M. Benzke, S. J. Lee, M. Neubert and G. Paz, JHEP **1008**, 099 (2010) [arXiv:1003.5012 [hep-ph]].
27. M. Misiak *et al.*, Phys. Rev. Lett. **98**, 022002 (2007) [hep-ph/0609232].
28. T. Hermann, M. Misiak and M. Steinhauser, JHEP **1211**, 036 (2012) [arXiv:1208.2788 [hep-ph]].
29. A. Khodjamirian, T. Mannel, A. A. Pivovarov and Y.-M. Wang, JHEP **1009**, 089 (2010) [arXiv:1006.4945 [hep-ph]].
30. M. Beneke, G. Buchalla, M. Neubert and C. T. Sachrajda, Phys. Rev. Lett. **83** (1999) 1914 [hep-ph/9905312].
31. M. Beneke, T. Feldmann and D. Seidel, Nucl. Phys. B **612**, 25 (2001) [hep-ph/0106067].
32. A. Ali and A. Y. Parkhomenko, Eur. Phys. J. C **23**, 89 (2002) [hep-ph/0105302].
33. S. W. Bosch and G. Buchalla, Nucl. Phys. B **621**, 459 (2002) [hep-ph/0106081].
34. M. Beneke, T. Feldmann and D. Seidel, Eur. Phys. J. C **41**, 173 (2005) [hep-ph/0412400].
35. H. n. Li and H. L. Yu, Phys. Rev. D **53**, 2480 (1996) [hep-ph/9411308].
36. Y. Y. Keum, H. N. Li and A. I. Sanda, Phys. Rev. D **63**, 054008 (2001) [hep-ph/0004173].
37. Y. Y. Keum, M. Matsumori and A. I. Sanda, Phys. Rev. D **72**, 014013 (2005) [hep-ph/0406055].
38. C. D. Lu, M. Matsumori, A. I. Sanda and M. Z. Yang, Phys. Rev. D **72**, 094005 (2005) Erratum: [Phys. Rev. D **73**, 039902 (2006)] [hep-ph/0508300].
39. J. g. Chay and C. Kim, Phys. Rev. D **68**, 034013 (2003) [hep-ph/0305033].
40. T. Becher, R. J. Hill and M. Neubert, Phys. Rev. D **72**, 094017 (2005) [hep-ph/0503263].
41. A. Ali, B. D. Pecjak and C. Greub, Eur. Phys. J. C **55**, 577 (2008) [arXiv:0709.4422 [hep-ph]].
42. A. Ghinculov, T. Hurth, G. Isidori and Y. P. Yao, Nucl. Phys. B **685**, 351 (2004) [hep-ph/0312128].
43. H. H. Asatryan, H. M. Asatrian, C. Greub and M. Walker, Phys. Rev. D **65**, 074004

- (2002) [hep-ph/0109140].
44. A. Ali, E. Lunghi, C. Greub and G. Hiller, Phys. Rev. D **66**, 034002 (2002) [hep-ph/0112300].
 45. T. Huber, E. Lunghi, M. Misiak and D. Wyler, Nucl. Phys. B **740**, 105 (2006) [hep-ph/0512066].
 46. T. Huber, T. Hurth and E. Lunghi, Nucl. Phys. B **802**, 40 (2008) [arXiv:0712.3009 [hep-ph]].
 47. A. Ali, T. Mannel and T. Morozumi, Phys. Lett. B **273**, 505 (1991).
 48. F. Kruger and L. M. Sehgal, Phys. Lett. B **380**, 199 (1996) [hep-ph/9603237].
 49. T. Huber, T. Hurth and E. Lunghi, JHEP **1506**, 176 (2015) [arXiv:1503.04849 [hep-ph]].
 50. J. P. Lees *et al.* [BaBar Collaboration], Phys. Rev. Lett. **112**, 211802 (2014) [arXiv:1312.5364 [hep-ex]].
 51. Y. Sato *et al.* [Belle Collaboration], Phys. Rev. D **93**, no. 3, 032008 (2016) Addendum: [Phys. Rev. D **93**, no. 5, 059901 (2016)] [arXiv:1402.7134 [hep-ex]].
 52. A. Bharucha, T. Feldmann and M. Wick, JHEP **1009**, 090 (2010) [arXiv:1004.3249 [hep-ph]].
 53. E. Dalgic, A. Gray, M. Wingate, C. T. H. Davies, G. P. Lepage and J. Shigemitsu, Phys. Rev. D **73**, 074502 (2006) Erratum: [Phys. Rev. D **75**, 119906 (2007)] [hep-lat/0601021].
 54. C. M. Bouchard, G. P. Lepage, C. J. Monahan, H. Na and J. Shigemitsu, PoS LATTICE **2013**, 387 (2014) [arXiv:1310.3207 [hep-lat]].
 55. C. Bouchard *et al.* [HPQCD Collaboration], Phys. Rev. D **88**, no. 5, 054509 (2013) Erratum: [Phys. Rev. D **88**, no. 7, 079901 (2013)] [arXiv:1306.2384 [hep-lat]].
 56. J. A. Bailey *et al.* [Fermilab Lattice and MILC Collaborations], Phys. Rev. Lett. **115**, no. 15, 152002 (2015) [arXiv:1507.01618 [hep-ph]].
 57. M. Beneke and T. Feldmann, Nucl. Phys. B **592**, 3 (2001) [hep-ph/0008255].
 58. A. Ali, G. Kramer and G. h. Zhu, Eur. Phys. J. C **47**, 625 (2006) [hep-ph/0601034].
 59. R. Aaij *et al.* [LHCb Collaboration], Phys. Rev. Lett. **113**, 151601 (2014) [arXiv:1406.6482 [hep-ex]].
 60. C. Bobeth, G. Hiller and G. Piranishvili, JHEP **0712**, 040 (2007) [arXiv:0709.4174 [hep-ph]].
 61. C. W. Chiang, X. G. He and G. Valencia, Phys. Rev. D **93**, no. 7, 074003 (2016) [arXiv:1601.07328 [hep-ph]].
 62. G. Hiller and M. Schmaltz, Phys. Rev. D **90**, 054014 (2014) [arXiv:1408.1627 [hep-ph]].
 63. M. Bauer and M. Neubert, Phys. Rev. Lett. **116**, no. 14, 141802 (2016) [arXiv:1511.01900 [hep-ph]].
 64. R. Barbieri, G. Isidori, A. Pattori and F. Senia, Eur. Phys. J. C **76**, no. 2, 67 (2016) [arXiv:1512.01560 [hep-ph]].
 65. J. C. Pati and A. Salam, Phys. Rev. D **8**, 1240 (1973).
 66. J. C. Pati and A. Salam, Phys. Rev. D **10**, 275 (1974) Erratum: [Phys. Rev. D **11**, 703 (1975)].
 67. I. Dorsner, S. Fajfer, A. Greljo, J. F. Kamenik and N. Kosnik, arXiv:1603.04993 [hep-ph].
 68. R. Aaij *et al.* [LHCb Collaboration], JHEP **1602**, 104 (2016) [arXiv:1512.04442 [hep-ex]].
 69. R. Aaij *et al.* [LHCb Collaboration], JHEP **1307**, 084 (2013) [arXiv:1305.2168 [hep-ex]].
 70. S. Descotes-Genon, T. Hurth, J. Matias and J. Virto, JHEP **1305**, 137 (2013) [arXiv:1303.5794 [hep-ph]].

71. S. Jäger and J. Martin Camalich, JHEP **1305**, 043 (2013) [arXiv:1212.2263 [hep-ph]].
72. S. Jäger and J. Martin Camalich, Phys. Rev. D **93**, no. 1, 014028 (2016) [arXiv:1412.3183 [hep-ph]].
73. W. Altmannshofer and D. M. Straub, Eur. Phys. J. C **75**, no. 8, 382 (2015) [arXiv:1411.3161 [hep-ph]].
74. T. Hurth and F. Mahmoudi, JHEP **1404**, 097 (2014) [arXiv:1312.5267 [hep-ph]].
75. S. Descotes-Genon, L. Hofer, J. Matias and J. Virto, JHEP **1412**, 125 (2014) [arXiv:1407.8526 [hep-ph]].
76. A. Abdesselam *et al.* [Belle Collaboration], arXiv:1604.04042 [hep-ex].
77. M. Ciuchini, M. Fedele, E. Franco, S. Mishima, A. Paul, L. Silvestrini and M. Valli, JHEP **1606**, 116 (2016) [arXiv:1512.07157 [hep-ph]].
78. A. Ali, A. Y. Parkhomenko and A. V. Rusov, Phys. Rev. D **89**, no. 9, 094021 (2014) [arXiv:1312.2523 [hep-ph]].
79. C. G. Boyd, B. Grinstein and R. F. Lebed, Phys. Rev. Lett. **74**, 4603 (1995) [hep-ph/9412324].
80. C. Bourrely, I. Caprini and L. Lellouch, Phys. Rev. D **79**, 013008 (2009) Erratum: [Phys. Rev. D **82**, 099902 (2010)] [arXiv:0807.2722 [hep-ph]].
81. C. Hambrock, A. Khodjamirian and A. Rusov, Phys. Rev. D **92**, no. 7, 074020 (2015) [arXiv:1506.07760 [hep-ph]].
82. R. Aaij *et al.* [LHCb Collaboration], JHEP **1510** (2015) 034 [arXiv:1509.00414 [hep-ex]].
83. V. Khachatryan *et al.* [CMS and LHCb Collaborations], Nature **522**, 68 (2015) [arXiv:1411.4413 [hep-ex]].
84. C. Bobeth, M. Gorbahn, T. Hermann, M. Misiak, E. Stamou and M. Steinhauser, Phys. Rev. Lett. **112**, 101801 (2014) [arXiv:1311.0903 [hep-ph]].
85. T. Hermann, M. Misiak and M. Steinhauser, JHEP **1312**, 097 (2013) [arXiv:1311.1347 [hep-ph]].
86. C. Bobeth, M. Gorbahn and E. Stamou, Phys. Rev. D **89**, no. 3, 034023 (2014) [arXiv:1311.1348 [hep-ph]].
87. K. De Bruyn, R. Fleischer, R. Knegjens, P. Koppenburg, M. Merk, A. Pellegrino and N. Tuning, Phys. Rev. Lett. **109**, 041801 (2012) [arXiv:1204.1737 [hep-ph]].
88. S. Aoki *et al.*, Eur. Phys. J. C **74**, 2890 (2014) [arXiv:1310.8555 [hep-lat]].
89. A. J. Buras, F. De Fazio and J. Girrbach, JHEP **1402**, 112 (2014) [arXiv:1311.6729 [hep-ph]].